Available online at www.sciencedirect.com
ScienceDirect
Trans. Nonferrous Met. Soc. China 33(2023) 285−292

Transactions of Nonferrous Metals Society of China
www.tnmsc.cn

# Thermal decomposition of Bayan Obo mixed rare earth concentrate under inert atmosphere

De-liang MENG[1,2,3], Xiao-wei HUANG[1,2,3], Zong-yu FENG[1,4], Meng WANG[1,4], Chao XIA[1,4], Yan-yan ZHAO[1,4]

1. National Engineering Research Center for Rare Earth, GRINM Group Co., Ltd., Beijing 100088, China;
2. School of Metallurgy, Northeastern University, Shenyang 110819, China;
3. General Research Institute for Nonferrous Metals, Beijing 100088, China;
4. GRIREM Advanced Materials Co., Ltd., Beijing 100088, China

Received 15 October 2021; accepted 1 March 2022

**Abstract:** To provide basic research for the development and application of advanced technology for the metallurgy of Bayan Obo mixed rare earth concentrate (BOMREC), the thermal decomposition behavior of BOMREC under nitrogen atmosphere was investigated by using the Kissinger method, TGA−DSC and XRD etc., including the thermal decomposition kinetics, phase change, cerium oxidation efficiency, and phase change effect on the leaching efficiency of rare earth elements (REEs). The results indicate that during the roasting at 500−550 °C, the mass loss and activation energy ($E_a$) are approximately 10% and 148 kJ/mol, respectively. After roasting at 550 °C for 2 h, the bastnaesite in the BOMREC is completely decomposed and converted into rare earth oxides and fluorine oxides. The maximum oxidation efficiency of cerium reaches 0.58%. The maximum leaching efficiency of REEs reaches 49.1% after thermal decomposition at 600 °C for 2 h.

**Key words:** inert atmosphere; thermal decomposition; cerium oxidation; phase change; Bayan Obo mixed rare earth concentrate

## 1 Introduction

The Bayan Obo mixed rare earth concentrate (BOMREC) is defined as a critical rare earth resource that supplies more than 60% of the world's rare earth raw materials [1−3]. The rational development and utilization of BOMREC has a decisive influence on world rare earth patterns. At present, more than 90% of BOMRECs are treated by the third-generation sulfuric acid process due to the outstanding advantages of high rare earth recovery, low operating cost, strong adaptability and easy-to-achieve large-scale continuous production [4−6]. However, the current mainstream process in industry is facing environmental issues caused by the high output of waste gas and radioactive solid slag. In recent years, new advanced technologies have been proposed for the clean treatment of rare earth concentrates, such as the combination method [7], where BOMREC is successively treated by roasting decomposition, hydrochloric acid leaching and sulfuric acid roasting to greatly reduce the production of waste gas and residue from the source. In addition, some other advanced technologies, the oxidation roasting−sodium carbonate roasting process [8] and the acid leaching−alkali solution process containing roasting, hydrochloric acid leaching and alkali decomposition [9], have also been reported recently.

The thermal decomposition of rare earth concentrate without any additive, which is a critical

---

**Corresponding author:** Xiao-wei HUANG, Tel: +86-10-82241180, E-mail: hxw0129@188.com;
Zong-yu FENG, Tel: +86-10-82241180, E-mail: fengzongyu1120@163.com

DOI: 10.1016/S1003-6326(22)66106-5

operation unit of the new advanced technologies proposed in recent years, directly affects the leaching efficiency of rare earth elements (REEs) [10,11]. Previous studies indicated that during the thermal decomposition of rare earth concentrate in an oxidizing atmosphere, the trivalent cerium in the ore was easily oxidized to tetravalent cerium, which can be dissolved by inorganic acid in the form of a cerium−fluoride complex in the leaching process [12−14]. Unfortunately, in the hydrochloric acid system, the reaction between tetravalent cerium ions and chloride ions occurs easily in the leaching solution, and chlorine gas is generated, resulting in poisonous gas pollution [15,16]. It is a good way to solve the issue of chlorine gas pollution by inhibiting cerium oxidation during the thermal decomposition of rare earth concentrates. However, there are few studies on the thermal decomposition of BOMREC in inert atmospheres. Previous works reported that the bastnaesite in the mixed rare earth concentrate (66.54% REO) decomposed into (Ce, La)OF after roasting at 600 °C in an argon atmosphere for 2 h, and the cerium oxidation efficiency was 2.31% [17]. To better control the thermal decomposition of the mixed rare earth concentrate under an inert atmosphere, it is of great significance to systematically study the thermal decomposition kinetics, phase change and the effect of phase transformation on the leaching efficiency of REEs.

In this work, BOMREC is used as the raw material, and the reaction kinetics, phase change and cerium oxidation behavior during thermal decomposition in a nitrogen gas ($N_2$) atmosphere are studied. In addition, the effect of thermal decomposition behavior on the leaching efficiency of REEs is revealed. This work provides basic research for the development and application of advanced technology for treating BOMREC.

## 2 Experimental

### 2.1 Raw material and characterization

BOMREC was used as the experimental material in this work, and its chemical compositions are given in Table 1. The rare earth grade of the BOMREC was approximately 54 wt.% REO, and the light rare earth elements (La/Ce/Pr/Nd) accounted for more than 98 wt.% of the total rare earth elements in the BOMREC. In addition, the phase analysis of the raw material is shown in Fig. 1. The main phases of the raw material were monazite ($REPO_4$), bastnaesite ($REFCO_3$) and fluorite ($CaF_2$).

In addition, concentrated hydrochloric acid (analytically pure, Sinopharm Chemical Reagent Co., Ltd.) and deionized water with an electrical conductivity of <0.16 μS/cm were used in this work.

**Table 1** Chemical compositions of Bayan Obo mixed rare earth concentrate (wt.%)

| Rare earths | | | | | | | |
|---|---|---|---|---|---|---|---|
| $La_2O_3$ | $CeO_2$ | $Pr_6O_{11}$ | $Nd_2O_3$ | $Sm_2O_3$ | $Eu_2O_3$ | $Gd_2O_3$ | $Y_2O_3$ |
| 14.96 | 28.27 | 2.46 | 7.44 | 0.61 | 0.10 | 0.05 | 0.14 |
| Non-rare earths | | | | | | | |
| $Fe_2O_3$ | CaO | MgO | $MnO_2$ | F | P | $Al_2O_3$ | PbO |
| 4.61 | 5.57 | 0.20 | 0.08 | 9.18 | 3.74 | 0.04 | 0.28 |

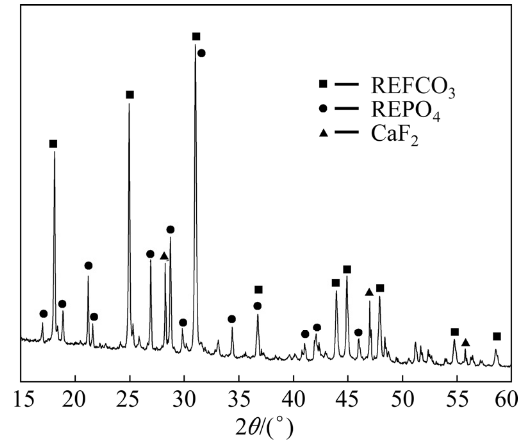

**Fig. 1** XRD pattern of Bayan Obo mixed rare earth concentrate

### 2.2 Experimental methods

First, 50 g of BOMREC was placed in a quartz boat (5 cm × 10 cm) and placed in a tube furnace. Before heating, $N_2$ gas with a flow rate of 500 mL/min was pumped into the tube furnace for approximately 30 min to empty the air in the furnace. Then, the sample was heated at a heating rate of 10 °C/min to the required temperature and roasted for 2 h. Finally, the roasted ore was cooled to room temperature in a $N_2$ atmosphere. During roasting and cooling, $N_2$ gas was continuously pumped into the tube furnace to maintain an inert atmosphere.

To obtain the kinetic data for the thermally induced process, the samples (approximately 9 mg) were heated in flowing dry $N_2$ gas (20 mL/min) from room temperature to 800 °C using the simultaneous thermogravimetry–differential thermal analysis (TGA−DSC 3+, Mettler Toledo International Co., Ltd.). TGA−DSC measurements were performed at various heating rates of 5, 10, 15 and 20 °C/min, respectively. In addition, the phase compositions of BOMRECs before and after roasting were analyzed by XRD with Cu $K_\alpha$ radiation (D8 Advance, Germany).

In this work, chemical analysis was used to determine the cerium oxidation efficiency of the roasted ores that were obtained at different roasting temperatures. The specific analysis process was described in the published literature [18].

To analyze the leaching efficiency of REEs in the roasted ore, a leaching experiment was carried out under the conditions of HCl (4.0 mol/L), liquid-to-solid ratio (20:1 mL/g), temperature (60 °C), reaction time (1 h) and agitation (300 r/min). After the leaching reaction, the slurry was filtered to obtain the filter cake and filtrate. The filter cake was dried at 100 °C in an oven for 12 h. ICP–OES (Optima 8300, Perkin Elemer, USA) was employed to characterize the chemical compositions of the leaching liquids.

### 2.3 Relevant calculation formulas

The kinetic parameters of the rare earth concentrate during decomposition were determined by the Kissinger method in this work, and the simplified form of Kissinger equation is shown as Eq. (1) when the order of reaction is 1 [19,20]:

$$\ln\left(\frac{\beta}{T_\mathrm{p}^{2}}\right)=\ln\left(\frac{AR}{E_\mathrm{a}}\right)-\frac{E_\mathrm{a}}{R}\cdot\frac{1}{T_\mathrm{p}} \tag{1}$$

where $\beta$ represents the heating rate ($\mathrm{d}T/\mathrm{d}t$), K/min; $T_\mathrm{p}$ is the exothermic peak temperature, K; $A$ is identified as the pre-exponential factor of the Arrhenius equation, $\mathrm{s}^{-1}$; $E_\mathrm{a}$ is the activation energy, kJ/mol; $R$ is molar gas constant, 8.314 J/(mol·K).

The leaching efficiency of rare earth elements is calculated according to Eq. (2):

$$\eta=\frac{m_1}{m_0}=\frac{C_1V_1}{w_0m_0}\times100\% \tag{2}$$

where $\eta$ is the leaching efficiency of rare earth elements (wt.%); $m_1$ is the mass of La, Ce, Pr, Nd, or REEs in the leaching solution; $m_0$ is the mass of La, Ce, Pr, Nd, or REEs in the mixed rare earth concentrate (g); $C_1$ is the concentration of La, Ce, Pr, Nd, or REEs in the leaching solution (g/L); $V_1$ is the volume of the leaching liquid (L); $w_0$ is the mass fraction of La, Ce, Pr, Nd, or REEs in the mixed rare earth concentrate (%).

The oxidation rate of Ce is calculated by

$$\varphi=\frac{m_{\mathrm{Ce(IV)}}}{m_{\mathrm{Ce(III)}}+m_{\mathrm{Ce(IV)}}}\times100\% \tag{3}$$

where $\varphi$ is the oxidation efficiency of Ce; $m_{\mathrm{Ce(IV)}}$ is the mass of Ce(IV) in the roasted concentrate (g), and $m_{\mathrm{Ce(III)}}$ is the mass of Ce(III) in the roasted concentrate (g).

## 3 Results and discussion

### 3.1 Kinetics of thermal decomposition

To obtain the kinetic parameters of the thermal decomposition of the mixed rare earth concentrate, the TG and DSC curves of the samples at different heating rates (5, 10, 15, and 20 °C/min) are shown in Figs. 2 and 3, respectively.

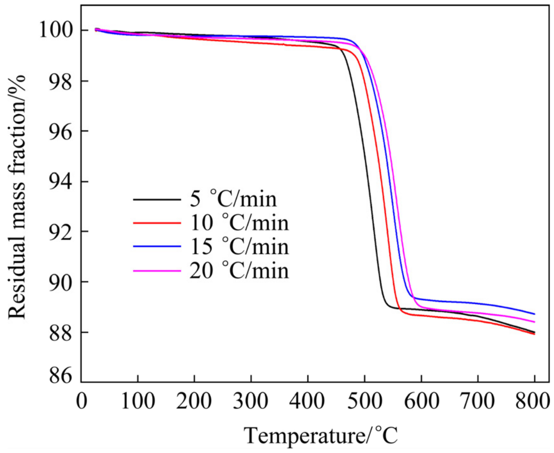

**Fig. 2** TG curves of BOMREC at different heating rates

From Fig. 2, as the heating rate increases, the TG curve moves to a higher temperature range, and only one steep slope due to mass loss of approximately 10 wt.% is found in each TG curve, which is caused by the release of $CO_2$ gas during the decomposition of bastnaesite in the mixed rare earth concentrate [21]. Accordingly, from Fig. 3, there is an obvious endothermic peak in each DSC curve, and the endothermic peak temperature ($T_\mathrm{p}$) increases with the heating rate. According to the DSC curves obtained at different heating rates, a curve of $\ln(\beta/T_p^2)$ versus $1/T_p$ is plotted, and a straight line is fitted to the data, as shown in Fig. 4. The activation energy ($E_a$=148 kJ/mol) and pre-exponential factor ($A$=7.9×10$^8$ s$^{-1}$) are calculated by the Kissinger equation described in Eq. (1). According to the activation energy obtained in this work, it can be concluded that the thermal decomposition reaction rate of the mixed rare earth concentrate at 450−600 °C is determined by chemical reaction [12]. Therefore, the thermal decomposition of the mixed rare earth concentrate can be promoted by properly increasing the roasting temperature, which provides theoretical guidance for optimizing roasting conditions.

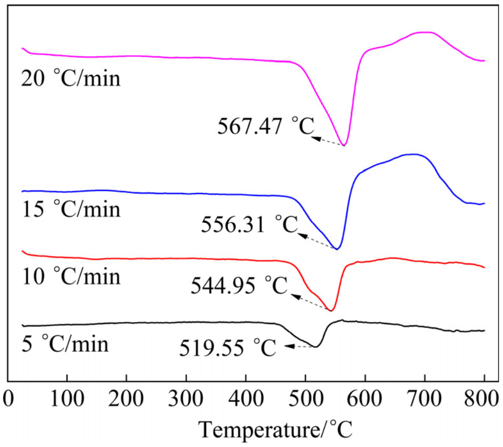

**Fig. 3** DSC curves of Bayan Obo mixed rare earth concentrate at different heating rates

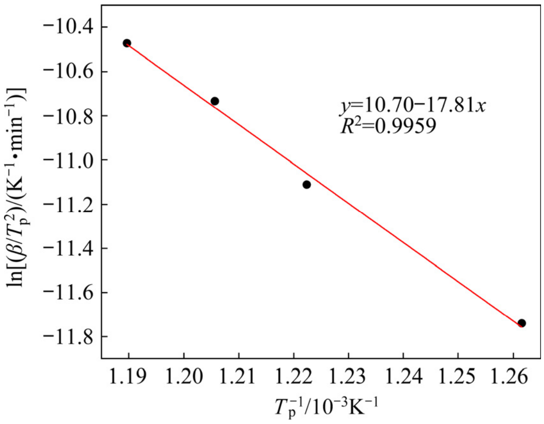

**Fig. 4** Fitting line of $\ln(\beta/T_p^2)$ versus $1/T_p$

### 3.2 Phase changes during thermal decomposition

To trace the phase changes during the decomposition process, the samples are roasted at different roasting temperatures (heating rate of 10 °C/min) for 2 h in a $N_2$ atmosphere, and the XRD patterns of the samples are analyzed in Fig. 5.

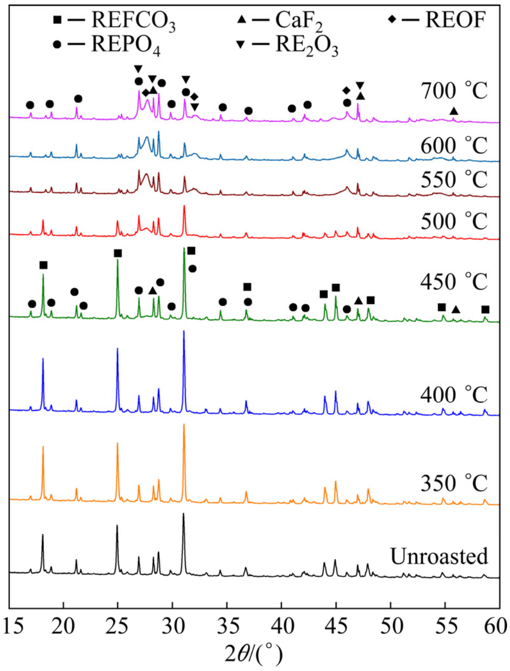

**Fig. 5** XRD patterns of roasted concentrates at different temperatures

When the roasting temperature is lower than 450 °C, the diffraction peak intensity corresponding to bastnaesite does not change significantly, and no new diffraction peak is found, indicating that bastnaesite in the mixed rare earth concentrate does not decompose. When the temperature reaches 500 °C, the diffraction peak of bastnaesite can still be detected, but the peak intensity is obviously weakened, indicating that bastnaesite has partially decomposed. At the same time, new phases ($RE_2O_3$, and REOF) are detected at this temperature, and this phenomenon can be explained by the decomposition reaction of bastnaesite in the mixed rare earth concentrate, as shown in Reactions (4) and (5). In addition, it has been reported that $CO_2$ gas, which is produced during the thermal decomposition of bastnaesite, can oxidize Ce(III) in bastnaesite even in an inert atmosphere according to the reaction described in Reaction (6) [18]. Therefore, in this work, cerium mainly exists in the form of Ce(III), but there is still a small amount of Ce(IV) in the generated rare earth oxides. Above 550 °C, the diffraction peak of bastnaesite could not be detected due to the complete decomposition of bastnaesite. The temperature (550 °C) for complete decomposition of bastnaesite in the mixed rare earth concentrate in a nitrogen atmosphere is higher than that (500 °C) in air atmosphere [22].

$$3REFCO_3=RE_2O_3+REF_3+3CO_2(g) \tag{4}$$

$$RE_2O_3+REF_3=3REOF \tag{5}$$

$$3CeOF+CO_2=2CeO_2+CeF_3+CO(g) \tag{6}$$

### 3.3 Ce oxidation behavior during thermal decomposition

To clarify the cerium oxidation behavior of the mixed rare earth concentrate during thermal decomposition in a $N_2$ atmosphere, the oxidation efficiency of cerium and mass loss rate are analysed, as shown in Fig. 6.

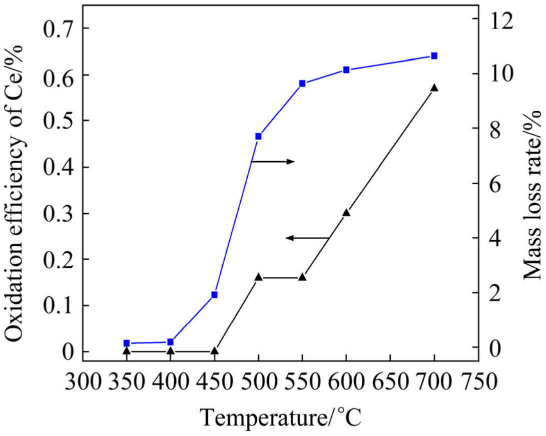

**Fig. 6** Oxidation efficiency of cerium and mass loss rate of mixed rare earth concentrate at different temperatures

When the calcination temperature is lower than 450 °C, no mass loss or cerium oxidation is detected because the samples do not decompose at this temperature. At 450 °C, a mass loss rate of approximately 2% is observed owing to the emission of $CO_2$ gas during the decomposition of bastnaesite in the mixed rare earth concentrate. In this case, no obvious oxidation of cerium occurs because very little $CO_2$ gas is produced at this temperature. From 500 to 550 °C, the mass loss increases significantly due to the thermal decomposition of bastnaesite in the mixed rare earth concentrate. A relatively low cerium oxidation efficiency of approximately 0.15% is detected. The reason is that the $CO_2$ concentration in the system is low because the generated $CO_2$ gas is continuously taken out of the system in this work, resulting in an indistinguishable change in cerium oxidation efficiency. From 550 to 700 °C, the mass loss rate tends to be stable at approximately 10%, but the oxidation efficiency of Ce is significantly improved from 0.15% to 0.58%. On the one hand, the cerium oxidation reaction described as Reaction (6) is thermally facilitated by increasing temperature [18]. On the other hand, according to the results of thermal decomposition kinetics, the decomposition rate of bastnaesite increases with increasing temperature; thus, the concentration of $CO_2$ in the system increases with the roasting temperature, resulting in a positive shift of the reaction equilibrium of Reaction (6).

In addition, it has been reported that cerium is also oxidized into Ce(IV) with a cerium oxidation efficiency of 2.31% during thermal decomposition of the mixed rare earth concentrate under an argon atmosphere [17], which is consistent with the result of this work. In comparison, during thermal decomposition in air atmosphere, the oxidation rate of cerium in the mixed rare earth concentrate can reach 60% [22].

### 3.4 Effect of phase change on rare earth leaching efficiency

To illustrate the influence of phase changes during thermal decomposition on the leaching efficiency of REEs, the samples prepared at different roasting temperatures are used as raw materials, and the leaching efficiency of REEs in the hydrochloric acid leaching process is shown in Fig. 7.

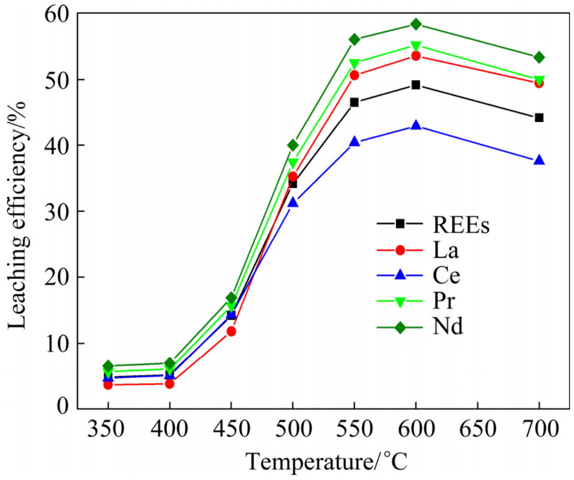

**Fig. 7** Leaching efficiency of rare earth elements in roasted ores obtained at different temperatures

When the roasting temperature is lower than 450 °C, the leaching efficiency of REEs is less than 5%. According to the results above in this work, the bastnaesite in the mixed concentrate does not decompose at temperatures below 450 °C, and only the REEs on the surface of the sample may be dissolved by hydrochloric acid. With increasing roasting temperature (450−600 °C), the leaching efficiencies of REEs (14.2%−49.1%), La (11.8%−53.5%), Ce (14.3%−42.9%), Pr (15.7%−55.2%), and Nd (16.9%−58.3%) increase significantly. However, when the roasting temperature continues to rise to 700 °C, the leaching efficiencies of REEs decrease slightly. The reason is that high temperature leads to the densification of the sample surface, resulting in insufficient solid–liquid contact during the leaching process [21].

To further analyze the leaching behavior of different phases in the roasted ore, the phase compositions and rare earth partition of the leaching residue are characterized in this work. Figure 8 exhibits the partitioning of La/Ce/Pr/Nd elements in the leaching residue. The proportion of La/Pr/Nd to the total REEs in the leaching residue tends to decrease, while that of Ce increases with increasing roasting temperature (450−550 °C). It can be inferred that insoluble compounds containing cerium (possibly $CeF_3$) are formed during the leaching process, resulting in the return of cerium to the leaching residue in the form of precipitates. The phase compositions of the rare-earth roasted ore and the leaching residue are compared to prove this point, as shown in Fig. 9. The main phases in the roasted ore are monazite ($REPO_4$), rare earth oxide (REO), rare earth fluoride oxide (REOF) and fluorite ($CaF_2$). In contrast, only two major phases of $REPO_4$ and $CeF_3$ are found in the leaching residue, which confirms that the phases of REO, REOF and $CaF_2$ are dissolved and that the precipitation of $CeF_3$ is generated during the leaching process. This phenomenon is in good agreement with the results of the relatively low leaching efficiency of Ce, as shown in Fig. 7.

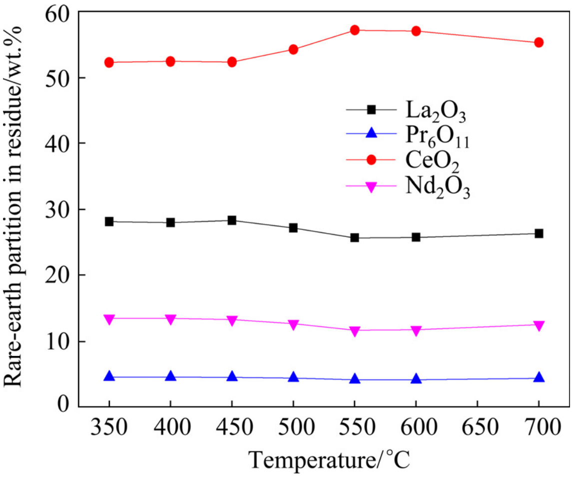

**Fig. 8** Proportion of La/Ce/Pr/Nd elements to total REEs in leaching residue of rare earth roasted ores obtained at different roasting temperatures

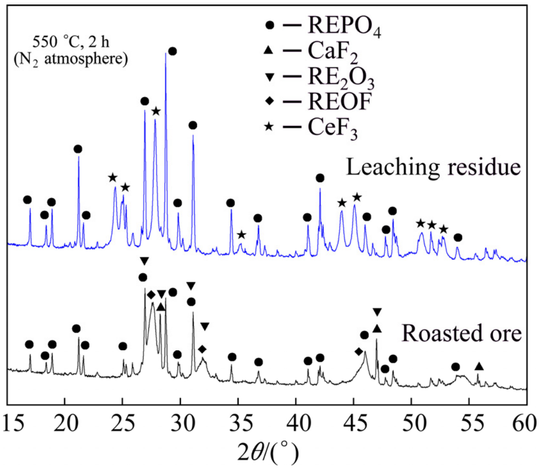

**Fig. 9** XRD patterns of roasted ore and leaching residue

## 4 Conclusions

(1) After the thermal decomposition of the Bayan Obo mixed rare earth concentrate in a $N_2$ gas atmosphere at 500−550 °C, the mass loss is approximately 10 wt.%, and the activation energy ($E_a$) is calculated to be equal to 148 kJ/mol.

(2) After roasting at 550 °C for 2 h, the bastnaesite in the Bayan Obo mixed rare earth concentrate can be completely decomposed, and new phases ($RE_2O_3$, and REOF) are generated simultaneously.

(3) During thermal decomposition in a $N_2$ gas atmosphere, a small amount of Ce(III) in the Bayan Obo mixed rare earth concentrate can still be oxidized to Ce(IV), and the maximum oxidation efficiency of Ce can reach 0.58%.

(4) The maximum leaching efficiency of REEs (49.1%) is obtained after thermal decomposition at 600 °C for 2 h in a nitrogen atmosphere, including La (53.5%), Ce (42.9%), Pr (55.2%) and Nd (58.3%). $CeF_3$ precipitates are formed during the leaching process, resulting in a relatively low leaching efficiency of cerium.

## Acknowledgments

This work was supported by the National Key Research and Development Program of

China (No. 2020YFC1909104), the Science and Technology Major Project of Guangxi, China (No. GuikeAA18242022), and the Key Research and Development Plan of Hebei Province, China (No. 20374104D).

## References

[1] HUANG Xiao-wei, LI Hong-wei, WANG Cai-feng, WANG Guo-zhen, XUE Xiang-xin, ZHANG Guo-cheng. Development status and research progress in rare earth industry in China [J]. Rare Metals, 2007, 31: 279−288. (in Chinese)

[2] FENG Zong-yu, HUANG Xiao-wei, WANG Meng, ZHANG Guo-cheng. Progress and trend of green chemistry in extraction and separation of typical rare earth resources [J]. Rare Metals, 2017, 41: 604−612. (in Chinese)

[3] HUANG Xiao-wei, LONG Zhi-qi, WANG Liang-shi, FENG Zong-yu. Technology development for rare earth cleaner hydrometallurgy in China [J]. Rare Metals, 2015, 34: 215−222.

[4] WANG Meng, HUANG Xiao-wei, FENG Zong-yu, LONG Zhi-qi, PENG Xin-lin, ZHANG Yong-qi. Progress and trend of green technology in the hydrometallurgy and separation of Bayan Obo mixed rare earth concentrate [J]. Rare Metals, 2019, 43: 1131−1141. (in Chinese)

[5] WANG Liang-shi, HUANG Xiao-wei, YU Ying, ZHAO Long-sheng, WANG Chun-mei, FENG Zong-yu, CUI Da-li, LONG Zhi-qi. Towards cleaner production of rare earth elements from bastnaesite in China [J]. Journal of Cleaner Production, 2017, 165(1): 231−242.

[6] CEN Peng, BIAN Xue, LIU Zhan-nian, GU Man-yi, WU Wen-yuan, LI Bao-kuan. Extraction of rare earths from bastnaesite concentrates: A critical review and perspective for the future [J]. Minerals Engineering, 2021. https://doi.org/10.1016/j.mineng.2021.107081.

[7] HUANG Xiao-wei, FENG Zong-yu, SUN Xu, XU Yang, WANG Meng, WANG Liang-shi, XIA Chao, LIU Xiang-sheng, ZHAO Long-sheng, ZHANG Yong-qi. A smelting and separation process for rare earth concentrates treated by a combined method: Chinese patent, CN201980052517.6 [P]. 2019−08−09.

[8] ZHAO Jun-mei, PAN Feng, LIU Hui-zhou. An environmental friendly $Na_2CO_3$-roasting decomposition strategy for the mixed rare earth concentrate [J]. Separation and Purification Technology, 2016, 168: 161−167.

[9] LIU Xing-yu, HUANG Lan, LIU Zhao-gang, ZHANG Dong-liang, GAO Kai, LI Mei. A novel, clean, closed-loop process for directional recovery of rare earth elements, fluorine, and phosphorus from mixed rare earth concentrate [J]. Journal of Cleaner Production, 2021. https://doi.org/10.1016/j.jclepro.2021.128784.

[10] XIE Feng, ZHANG Ting-an, DREISINGER D, DOYLE F. A critical review on solvent extraction of rare earths from aqueous solutions [J]. Minerals Engineering, 2014, 56: 10−28.

[11] ZOU Dan, CHEN Ji, LI Kai, LI De-qian. Phase transformation and thermal decomposition kinetics of a mixed rare earth concentrate [J]. ACS Omega, 2018, 3(12): 17036−17041.

[12] BIAN Xue, CHEN Jian-li, ZHAO Zhi-hua, YIN Shao-hua, LUO Yao, ZHANG Feng-yun, WU Wen-yuan. Kinetics of mixed rare earths minerals decomposed by CaO with NaCl−$CaCl_2$ melting salt [J]. Journal of Rare Earths, 2010, 28: 86−90.

[13] FENG Xing-liang, LONG Zhi-qi, CUI Da-li, WANG Liang-shi, HUANG Xiao-wei, ZHANG Guo-cheng. Kinetics of rare earth leaching from roasted ore of bastnaesite with sulfuric acid [J]. Transactions of Nonferrous Metals Society of China, 2013, 23: 849−854.

[14] LI Mei, ZHANG Dong-liang, YAN Yu-jun, GAO Kai, LIU Xing-yu, LI Jian-fei. Effect of oxidation behavior of cerium during the roasting process on the leaching of mixed rare earth concentrate [J]. Hydrometallurgy, 2017, 174: 156−166.

[15] SHUAI Geng-hong. Study on reaction mechanism of the oxidation roasting and hydrochloric process involving acid leaching of bastnaesite [D]. Beijing: General Research Institute for Nonferrous Metals, 2017. (in Chinese)

[16] MENG De-liang, FENG Zong-yu, YANG Juan-yu, WANG Meng, XIA Chao, ZHAO Yan-yan, XU Yang, HUANG Xiao-wei. Reaction between $Ce^{4+}$ ion and thiourea in aqueous HCl medium: An electrochemical study [J]. Journal of the Electrochemical Society, 2021. https://doi.org/10.1149/1945-7111/ac1b4f.

[17] ZHANG Dong-liang. Basic research on acid leaching behavior of $Ce^{3+}$/$Ce^{4+}$ in mixed rare earth concentrates and conversion of fluoride and calcium resources [D]. Beijing: Beijing University of Chemical Technology, 2019. (in Chinese).

[18] ZHAO Long-sheng, WANG Liang-shi, SHUAI Geng-hong, LONG Zhi-qi, CUI Da-li, HUANG Xiao-wei. Thermal decomposition and oxidation of bastnaesite concentrate in inert and oxidative atmosphere [J]. Journal of Rare Earths, 2018, 36: 758−765.

[19] BLAINE R L, KISSINGER H E. Homer Kissinger and the Kissinger equation [J]. Thermochimica Acta, 2012, 540: 1−6.

[20] ZHANG Ting-an, DOU Zhi-he. Research methods for macrokinetics [M]. Beijing: Beijing Industrial Press, 2014. (in Chinese)

[21] XU Guang-xian. Rare earths [M]. 2nd ed. Beijing: Metallurgical Industry Press, 1995. (in Chinese)

[22] MENG De-liang, WANG Meng, FENG Zong-yu, XIA Chao, ZHAO Yan-yan, HUANG Xiao-wei. Behavior of phase transformation of Baotou mixed rare earth concentrate during oxidation roasting [J]. Journal of Rare Earths, 2021. https://doi.org/10.1016/j.jre.2021.04.004.

# 白云鄂博混合型稀土精矿在惰性气氛下的热分解行为

孟德亮 1,2,3，黄小卫 1,2,3，冯宗玉 1,4，王 猛 1,4，夏 超 1,4，赵岩岩 1,4

1. 有研科技集团有限公司 稀土国家工程研究中心，北京 100088；
2. 东北大学 冶金学院，沈阳 110819；
3. 北京有色金属研究总院，北京 100088；
4. 有研稀土新材料股份有限公司，北京 100088

**摘 要**：为了开发和应用白云鄂博混合型稀土精矿的先进冶炼技术，采用 Kissinger 公式、TGA−DSC 和 XRD 等分析方法，研究在氮气氛下白云鄂博混合型稀土精矿的热分解行为，包括热分解动力学、物相变化规律、铈氧化效率以及物相变化对稀土浸出率的影响。结果表明：在 500~550 ℃焙烧时，焙烧质量损失率约 10%、热分解活化能($E_a$)为 148 kJ/mol。550 ℃焙烧 2 h，白云鄂博混合型稀土精矿中氟碳铈矿完全分解，并转化为稀土氧化物和氟氧化物，铈氧化率最大值为 0.58%。600 ℃焙烧 2 h，稀土最大浸出率达 49.1%。

**关键词**：惰性气氛；热分解；铈氧化；物相变化；白云鄂博混合型稀土精矿

**(Edited by Bing YANG)**